

# PARP in DNA Damage Repair

Subjects: Biochemistry & Molecular Biology

Contributor: Lotte van Beek, Éilís McClay

Poly (ADP-ribose) polymerases (PARP) 1-3 are well-known multi-domain enzymes, catalysing the covalent modification of proteins, DNA, and themselves. They attach mono- or poly-ADP-ribose to targets using NAD<sup>+</sup> as a substrate. Poly-ADP-ribosylation (PARylation) is central to the important functions of PARP enzymes in the DNA damage response and nucleosome remodelling. Activation of PARP happens through DNA binding via zinc fingers and/or the WGR domain. Modulation of their activity using PARP inhibitors occupying the NAD<sup>+</sup> binding site has proven successful in cancer therapies. For decades, studies set out to elucidate their full-length molecular structure and activation mechanism.

Keywords: Poly (ADP-ribose) polymerases 1-3 ; DNA damage response ; PARP-DNA binding ; PARP activation

---

## 1. Introduction

Poly ADP-ribose polymerase (PARP) enzymes play a key role in a number of cellular processes, such as DNA repair, genome maintenance, and cell death <sup>[1][2][3][4][5][6][7]</sup>. The best characterised member of the PARP family is PARP1, which was first identified for its role in the recognition and repair of single-strand DNA breaks (SSB) <sup>[8][9]</sup>. Since then, PARP1 has also been shown to have a role in a number of DNA damage response (DDR) pathways, including base excision repair (BER), homologous recombination (HR), non-homologous end joining (NHEJ), and DNA mismatch repair. Consequently, PARPs have been an attractive target for anti-cancer therapies resulting in the successful development of several PARP inhibitors (PARPi) for ovarian, breast, lung, and pancreatic cancers <sup>[10]</sup>. This novel class of therapies competes with the native substrate nicotinamide adenine dinucleotide (NAD<sup>+</sup>) for the PARP catalytic site <sup>[11][12][13][14][15]</sup>.

It has been more than half a century since the discovery of PARP1 and the process of poly-ADP-ribosylation (PARylation) that PARP1, and other members of the PARP family, catalyse <sup>[1][2][3]</sup>. During PARP catalysis ADP-ribose residues are transferred from NAD<sup>+</sup> onto the target substrate building a poly ADP-ribose (PAR) chain. The building of PAR chains, along with their removal, occurs in all three major divisions of life (eukaryotes, prokaryotes, archaea) <sup>[16][17][18]</sup>. Here, we discuss the human enzymes in the context of DNA damage repair. The identification of PAR and its structure, and the realisation that PARP1 produces PAR, were key breakthroughs during early PARP research <sup>[19][20][21][22]</sup>. Studies that followed detailed the purification of PARP1 <sup>[23]</sup>, demonstrated the activation of PARP in response to genotoxic agents <sup>[8]</sup> <sup>[24]</sup>, linked PARP1 to the repair of DNA damage <sup>[9]</sup>, and showed the association of PAR with nucleosome remodelling and enzymes, including PARP1 itself <sup>[21][25]</sup>. Furthermore, the discovery of PARP2—and other members of the PARP family—was enabled by the generation and characterisation of the *PARP1* knockout mouse <sup>[26][27][28]</sup>.

The PARP family consists of 17 proteins in humans. PARP1, PARP2, PARP5A, and PARP5B are capable of synthesising PAR chains <sup>[1][2][3]</sup>. Most other members in the PARP family catalyse the addition of single ADP-ribose units and are therefore classified as mono ADP-ribosyltransferases (MARs). PARP1, PARP2, and PARP3 are DNA-dependent enzymes <sup>[4]</sup>. PARP1, the largest of the three, is approximately 116 kDa <sup>[29]</sup> and comprises of six independently folded domains: the N-terminus consists of three zinc (Zn) finger domains Zn1, Zn2, and Zn3; this is followed by the auto-modification domain, which contains the BRCA1 C-terminus (BRCT) fold and mediates protein–protein interactions; adjacent to this is the tryptophan, glycine, arginine (WGR) motif; whilst at the C-terminus sits the catalytic (CAT) domain ([Figure 1](#)) <sup>[30][31][32][33]</sup>. Four of these domains (Zn1, Zn2, Zn3, and WGR) have been shown to bind DNA ([Figure 1B](#)) <sup>[34]</sup>. The CAT domain is the most conserved across the PARP family and comprises of the helical subdomain (HD) and the ADP-ribosyl transferase (ART) subdomain ([Figure 1C](#)) <sup>[30][31]</sup>. Interestingly, PARP2 and PARP3 only share the C-terminal regions (WGR and CAT domains), yet they are able to regulate the mechanism of DNA-induced activation via local destabilisation of the HD. It has been proposed that human PARP2 contains an additional N-terminal DNA and/or RNA-binding domain <sup>[35][36][37]</sup>: the SAP motif named after the proteins in which it was found, SAF/Acinus/PIAS <sup>[38]</sup>. This motif occurs one to four times at the N-terminus of plant PARP2 <sup>[39][40]</sup> and is a putative DNA-binding four-helix bundle <sup>[41]</sup>. However, Riccio et al. (2015) <sup>[42]</sup> report that although the N-terminus of PARP2 is important for PARP2 activation on SSBs, the N-terminal region of human

PARP-2 is intrinsically disordered [42]. Therefore, here the SAP motif is not included in the domain overview of PARP2 (Figure 1A).

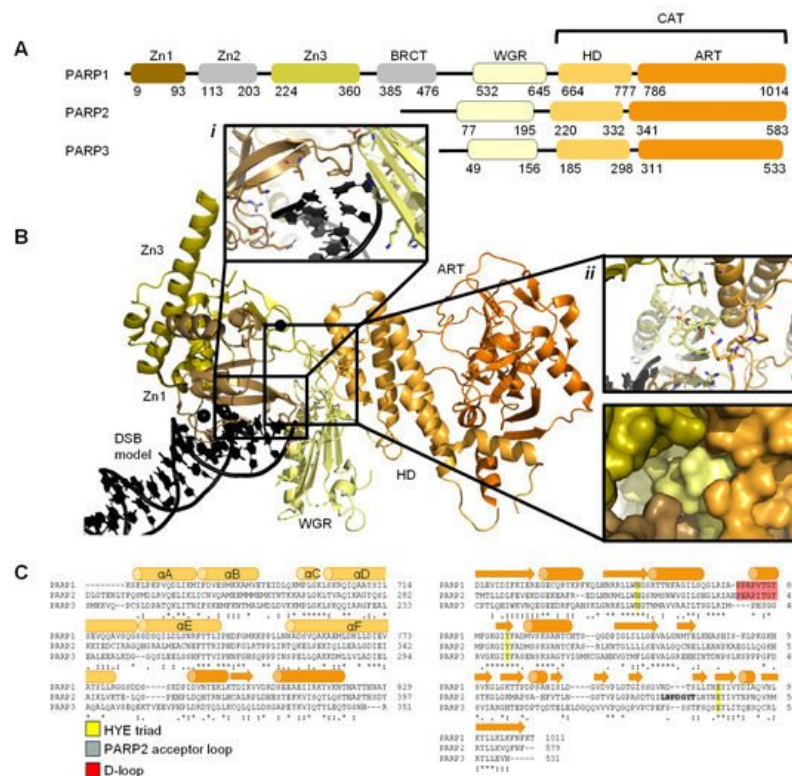


**Figure 1.** Overview of PARP1, PARP2, and PARP3. (A). Schematic overview of the domains of PARP1, PARP2, and PARP3, with amino acid numbers indicating domain boundaries corresponding to Uniprot entries P09874, Q9UGN5, and Q9Y6F1; (B). Crystal structure of PARP1 bound to a double-strand DNA molecule representing one end of a double-strand break (DSB) (Protein Data Bank (PDB) entry 4DQY [34]). Domain colours correspond to A. Inset *i*: interactions of Zn1 and WGR with a DSB model. Inset *ii*: interdomain interactions between Zn1, Zn3, WGR, and HD shown as cartoons (top) and surface representations (bottom). All figures in this review containing protein structures were generated in PyMOL [43]; (C). Structure-based sequence alignment of CAT domains of PARP1, PARP2, and PARP3 was generated in PyMOL [43]. Sequence alignment was generated in Clustal Omega [44] provided by EMBL-EBI [45]. Secondary structure is represented by cylinders as  $\alpha$ -helices and arrows as  $\beta$ -sheets, respectively. Sequence conservation is shown, where an asterisk represents fully conserved, a colon represents strongly similar properties and a period represents weakly similar properties. The conserved histidine, tyrosine, glutamic acid (HYE) triad is shown in yellow, the PARP2 acceptor loop in grey, and the D-loop in red.

Early structures of individual PARP domains were first published in the late 1990s for PARP1 [46][47][48], and early 2000s for PARP2 [49]. The first crystal structure of the human PARP1 CAT domain bound to a small molecule inhibitor was published by Kinoshita and co-workers in 2004 [50], and subsequently, for PARP2 by Karlberg et al. (2010) [51] and for PARP3 by Lehtiö and colleagues [52]. Thereafter, many more structures have been published of PARP1-3, often of individual domains and short truncated forms of the proteins. To date there have been no reported structures of full-length PARP1. However, the full-length structure of PARP2 and histone PARYlation factor 1 (HPF1) in complex with a nucleosome was recently determined by cryo-electron microscopy (cryo-EM) [53].

## 2. DNA Damage Recognition by PARP Enzymes

Each cell within an organism faces a high frequency of DNA damage on a daily basis [54][55], due to many endogenous and exogenous causes [56]. Members of the PARP family are key initiators of the DDR pathway amongst other functions [4][9][57]. Repairing damaged DNA is essential for cells to enable successful transcription, maintain genomic stability, achieve cell replication, and survive [56]. The majority of DNA damage within cells is inflicted on just one DNA strand and is known as a single strand break (SSB). These SSBs are often easier to repair given the necessary information is still available on the complementary strand. Different types of SSB damage can occur depending on the process which resulted in the break. For example, a DNA strand can be nicked (both bases are intact but the DNA backbone is broken), the pyrimidine/purine group can be missing resulting in an abasic (AP) site, or a nucleotide can be missing (gap) [54]. Double-strand breaks (DSBs) are more problematic for cells and therefore cells have dedicated pathways to rectify this type of

damage. Depending on the cell cycle stage, and the presence of a template, the HR or the NHEJ pathways are initiated [10][58].

PARPs play an essential role as DNA damage sensors, of both SSBs and DSBs [5], and promote DNA repair through recruitment of DNA repair factors. Examples of such PARP1 interactors include: the X-ray repair cross complementing group 1 (XRCC1) [59] acting as a scaffold for DNA SSB repair components; the tyrosyl-DNA phosphodiesterase 1 (TDP1) [60], which removes stalled topoisomerase 1 (TOP1)-DNA complexes; DNA protein kinase catalytic subunit (DNAPKcs) [61] in the NHEJ DSB repair pathway and variable, diversity, and joining (V(D)J) recombination [62]; the kinase ataxia telangiectasia mutated (ATM) [63][64] in DNA DSB repair; and the nuclease meiotic recombination 11 (MRE11), also in DSB repair [65][66].

## 2.1. PARP1 Zn Fingers Bind a DNA Break

Individual PARP1 domains Zn finger 1 (Zn1) or Zn finger 2 (Zn2) can both bind to DNA with a C $\alpha$  root mean square deviation (RMSD) of 0.96 Å, when a double-strand DNA molecule representing one end of a DSB is used as a model for DNA damage (PDBs 3ODA, 3ODC, Figure 2A [67]). Ali and colleagues [68] solved the crystal structure of a protein construct containing both Zn1 and Zn2 connected by their linker on a DSB model (PDB 4AV1). This shows Zn1 and Zn2 cooperate to recognise the DSB model (Figure 2B) yet their binding modes are very similar with a C $\alpha$  RMSD of 0.80 Å. Zn1 and Zn2 contact DNA at two locations in the phosphate backbone grip (Inset *i* in Figure 2A,B) through R18 (Zn1) or R122 (Zn2) and at the base stacking loop (Inset *ii* in Figure 2A,B) via F44 (Zn1) or L161/I164 (Zn2). In the cooperative interaction these base stacking interactions enhance each other. This happens through hydrophobic protein-DNA interactions mediated by L161/I164 from Zn2 capped with F44 from Zn1. This implicates the Zn finger regions of PARP1 in the binding, and subsequent repair, of DSBs.

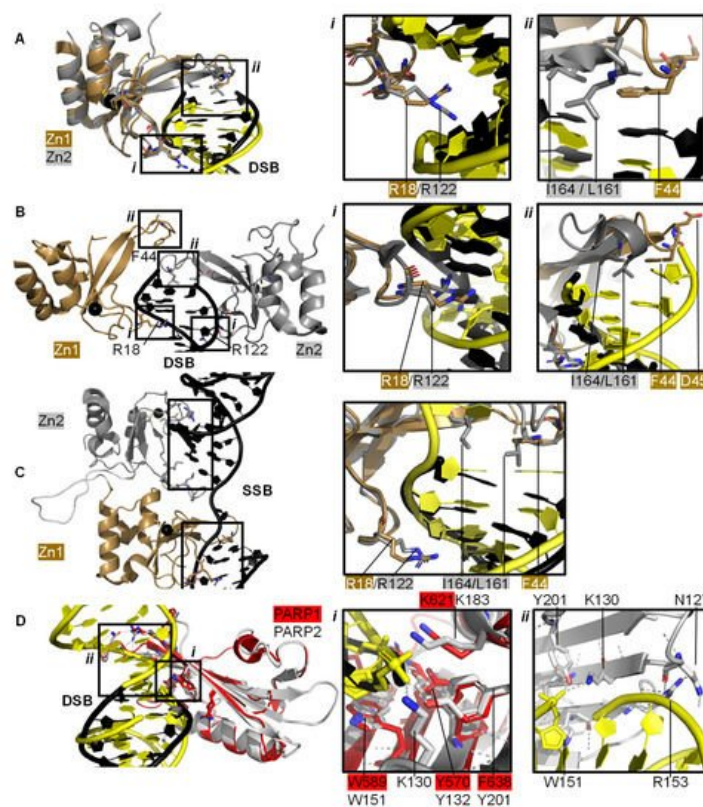


**Figure 2.** PARP domains in complex with a DNA DSB model (A,B), SSB (C), or DSB (D). (A) Superposed crystal structures of Zn fingers 1 (Zn1, brown, PDB 3ODA [67]) and 2 (Zn2, silver, PDB 3ODC [67]), RMSD 0.96 Å, in complex with DSB models shown in black for Zn1 and yellow for Zn2. Inset *i* shows the phosphate backbone grip and inset *ii* the base stacking loop; (B) Zn1 (brown) and Zn2 (silver) cooperate DSB model binding (PDB 4AV1 [68]). Insets show the superposition of Zn1 and Zn2 with an RMSD of 0.80 Å of the boxed regions. In the superposition, Zn1 and Zn2 binding to a DSB model is shown in black and yellow, respectively, where *i* shows the Zn finger loop with R18/R122 interacting with the major groove of the DSB model and *ii* the base stacking loop with F44/L161/I164; (C) Zn1 and Zn2 also cooperate SSB binding (PDB 2N8A [69]). Inset shows the superposition of the boxed regions in Zn1 and Zn2 on a SSB with an RMSD of 0.83 Å, where DNA in yellow binds to Zn1 and DNA in black binds to Zn2; (D) Superposition of the WGR domains from PARP1 (red, PDB 4DQY [34]) on a black DSB model and PARP2 (white, PDB 6F5B [70]) bridging a yellow DSB with a 5' phosphate group (C $\alpha$  RMSD of 0.89 Å). Inset *i* highlights the superposed WGR PARP1 and PARP2 residues involved in DNA binding. Inset *ii* shows how the WGR of PARP2 interacts with the second DSB using R153.

Both Zn finger interactions are sequence-independent as demonstrated in [Figure 2](#) and the nuclear magnetic resonance spectroscopy (NMR) structures of Zn finger domains (from PARP1 in absence of DNA overlaid with the protein-DNA complex structures [\[74\]](#)). This shows movement of the base stacking loop of Zn1 upon binding to DNA. Further DNA binding studies imply that the phosphate backbone grip of both Zn1 and Zn2 is key to DNA binding and the base stacking loop contributes modest complementary DNA binding ability. However, only Zn1 is essential for PARP1 activation or PARylation. This “activator” difference is attributed to the sequence diversity between Zn1 and Zn2 surrounding the base stacking loop. A D45A mutation in Zn1, which does not have an equivalent residue in Zn2 in the structure-based sequence alignment, abolishes inter-domain communication within PARP1 leading to PARylation, but this mutation does not prevent DNA binding. This is explained by the fact that D45 in Zn1 points away from the DNA-binding interface and so D45 in Zn1 is essential for inter-domain activation of PARP1 ([Figure 2B](#), inset *ii*). Furthermore, an equivalent residue is absent in Zn2, which explains why Zn2 cannot activate PARP1 on its own [\[67\]](#).

Eustermann et al. (2011) showed that Zn1 and Zn2 can both bind SSBs in structures obtained by NMR [\[71\]](#). The double domain construct Zn1-Zn2 with a flexible 15 amino acid linker binds the SSB model mainly using its Zn2 in a similar manner to Zn2 alone, confirming that Zn2 binds a SSB in preference to Zn1 [\[71\]](#). The structural rationale for this was explained by the solution structure of Zn1-Zn2 on a SSB ([Figure 2C](#)) [\[69\]](#). Zn2, the domain with a higher binding affinity for DNA, first senses the DNA SSB and interacts with the more accessible 3' site. This poises Zn1 for DNA binding to the more cryptic 5' site thereby twisting the DNA; a binding mode only accessible for SSBs. Zn1 and Zn2 also mediate cooperative binding through a hydrophobic interdomain interface ([Figure 2C](#)) [\[69\]](#). Remarkably, the key residues for interactions with both SSBs and DSBs are conserved and located in the phosphate backbone grip and base stacking loop. This is a testament to the flexibility of Zn finger domains in PARP1 in binding to different DNA break architectures.

The crystal structure of Zn finger 3 of PARP1 (Zn3, PDB 2RIQ) revealed a Zn finger fold different from Zn1/Zn2 [\[22\]](#). Zn3 uses its N-terminal  $\alpha$ -helical region to interact with the minor groove of DSBs [\[34\]](#). Destabilisation of Zn3 (by the introduction of negative charges in the Zn finger domain structure) resulted in a full-length PARP1 mutant able to bind DNA. However, this was unable to undergo DNA-dependent activation [\[72\]](#) suggesting that a function of Zn3 is to mediate interdomain contacts upon PARP1 activation by DNA binding. This is confirmed by detailed studies into the order of DNA interaction and PARP1 activation [\[34\]\[69\]](#), which describe how DNA binding initiates cooperative interdomain interactions between Zn3 and WGR that support destabilisation of the HD.

The 3.25 Å structure showing the minimal combination of PARP1 domains essential for PARP1 activation on a DSB model comprises Zn1, Zn3, WGR, and the HD-CAT domains [\[34\]](#), even though Zn2 can bind DSB models in an analogous fashion to Zn1 (PDB 4DQY, [Figure 1B](#)). Here, Zn1 and Zn3 make adjacent interactions to the ribose phosphate backbone of a DSB. They interact with the WGR domain central to PARP1, which binds the 5' terminus of the DSB via a range of aromatic and positively charged residues in the central  $\beta$ -sheet and Lys600 in its  $\alpha$ -helix, and mediates contacts to the CAT domain ([Figure 1B](#), inset *ii*) [\[34\]](#). The full-length structure of PARP1 on a DSB remains elusive.

## 2.2. Recognition and Binding of Other DNA Breaks via PARP Domains

PARP2 and PARP3 lack the Zn finger domains yet still recognise specific DNA breaks featuring 5' phosphate groups and subsequently initiating a DDR [\[57\]\[70\]\[73\]\[74\]](#). Here, the interaction with DNA is mediated by the WGR domain that is also present in PARP1 ([Figure 2D](#)). The structure of PARP2 shows similar binding modes for DNA with (PDB 6F5B) and without (PDB 6F1K) 5' phosphate group [\[70\]](#) despite preferentially binding damaged DNA featuring a 5' phosphate group [\[57\]](#). The key interaction in the PARP2-5' P-DNA appears to be Y201, which coordinates a hydrogen bond to the 5' phosphate group in PDB 6F5B ([Figure 2D](#), inset *i*), together with the lysine residues K130 and K183. In both structures the PARP2 WGR bridges a DSB ([Figure 2D](#), inset *ii*)—a feasible model of the physiological interaction of the DNA-binding recruitment domain of DNA damage sensor PARP2.

In addition, the N-terminus of PARP2 bears DNA-binding activity and assists in the activation of PARP2 on SSBs [\[42\]](#). This region also activates PARP2 in the presence of single-strand RNA molecules, but not double-strand DNA molecules [\[36\]](#).

## 2.3. The PARP Paradox: Finding a Needle in a Haystack

For effective DNA damage sensing, PARP molecules need to swiftly locate damaged DNA within a highly crowded nuclear environment containing lots of intact DNA: the estimated DNA concentration in the nucleus is 100 mg/mL [\[28\]\[29\]](#). A contributing factor to this is the high nuclear concentration of PARP molecules and in particular PARP1 [\[29\]\[75\]](#), estimated to 7–200  $\mu$ M from  $2 \times 10^5$ – $10^6$  copies of PARP1 per nucleus [\[29\]\[75\]](#), a cell volume between 100 and 10,000  $\mu$ m<sup>3</sup> [\[76\]](#) and a ratio of nuclear-to-cell volume of 0.08 [\[77\]](#). These PARP molecules have a very high binding affinity (low binding constant,  $K_D$ ) for damaged DNA, ranging from 3 to 62 nM depending on the PARP molecule and DNA damage site [\[78\]\[79\]](#), as

measured by Sukhanova et al. (2019) by atomic force microscopy (AFM). In this study, competitive binding was revealed between different members of the PARP family for similar binding sites on DNA. PARP1 has the highest affinity for nick sites, followed by nucleotide break sites and had the lowest affinity for abasic/aprimidinic (AP) sites. In contrast, PARP2 had similar affinity for nicked and AP sites and the lowest affinity for nucleotide break sites [79]. This confers an intrinsic difference in DNA binding mechanism, as might be expected with PARP2 lacking DNA-binding Zn domains. AFM binding experiments combined with protein volume measurements provided some insight into the observed oligomeric state of PARP molecules on damaged DNA. PARP1 was mostly monomeric on intact, AP sites and gaps with minute dimer formation on nicked sites, while PARP2 preferentially dimerised on gaps and nicked sites and was monomeric on intact and AP sites [79]. Studies are emerging on the molecular activation mechanism of PARP2 on DSBs.

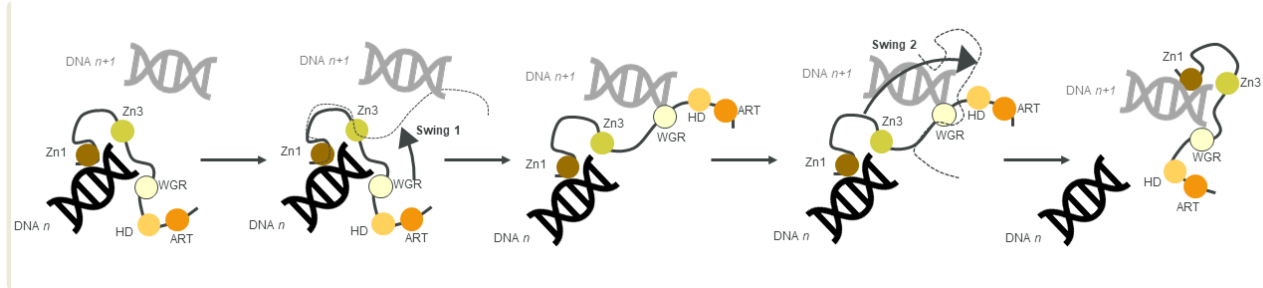


**Figure 3.** A schematic of the monkey bar mechanism, showing how PARP1 recognises DNA damage.

Another contribution to swift DNA damage sensing comes from the way PARP1 travels along intact DNA—termed the monkey bar mechanism (Figure 3) [80]. This intersegment transfer mode is estimated to enhance the ability of PARP1 to sense DNA damage threefold, compared to diffusion alone [81] (from stopped-flow experiments of PARP1 WT and a W589A mutant unable to use the monkey bar mechanism) [80][81]. Moreover, Rudolph et al. (2018) showed that since the association of PARP1 with DNA is faster than diffusion, PARP1 would struggle to release undamaged DNA once bound [80]. Instead, PARP1 makes good use of excess DNA in the nucleus by dissociating the lower-affinity DNA binding domain WGR from the originally bound DNA-molecule  $n$ . Due to the high DNA concentration in the nucleus, the WGR domain will bind to another DNA-molecule  $n + 1$ . This WGR-DNA interaction is primarily mediated through W589 (Figure 2D, inset *i*), which stacks against the ribose sugar of the 5' strand of DNA. When the stronger DNA-binding Zn finger domains dissociate from DNA  $n$  they will rapidly bind DNA  $n+1$ . This transfer enables PARP1 to quickly move between DNA molecules, most of which are undamaged until it finds a DNA break, where the Zn domains make specific interactions with the DNA break [31]. After a conformational change within PARP1, which is most likely pinpointed to the “closure” of the WGR onto DNA that happens on a slower timescale than binding of the Zn fingers to DNA [81], the HD domain gets destabilised and mediates allosteric activation of the catalytic domain of PARP1. This in turn strengthens the affinity of the Zn finger domains for the DNA break [32]. In summary, the tailored affinity of different members of the PARP family for different DNA breaks, swinging between high- and lower-affinity DNA-binding domains, and the sheer number of PARP molecules in the nucleus, are the clue towards finding the DNA strand break needle in the DNA haystack called the nucleus.

## References

- Gibson, B.A.; Kraus, W.L. New Insights into the Molecular and Cellular Functions of Poly(ADP-Ribose) and PARPs. *Nat. Rev. Mol. Cell Biol.* 2012, 13, 411–424.
- Kraus, W.L. PARPs and ADP-Ribosylation: 50 Years ... and Counting. *Mol. Cell* 2015, 58, 902–910.
- Cohen, M.S.; Chang, P. Insights into the Biogenesis, Function, and Regulation of ADP-Ribosylation. *Nat. Chem. Biol.* 2018, 14, 236–243.
- Barkauskaite, E.; Jankevicius, G.; Ahel, I. Structures and Mechanisms of Enzymes Employed in the Synthesis and Degradation of PARP-Dependent Protein ADP-Ribosylation. *Mol. Cell* 2015, 58, 935–946.
- Gupte, R.; Liu, Z.; Kraus, W.L. PARPs and ADP-Ribosylation: Recent Advances Linking Molecular Functions to Biological Outcomes. *Genes Dev.* 2017, 31, 101–126.
- Chaudhuri, A.R.; Nussenzweig, A. The Multifaceted Roles of PARP1 in DNA Repair and Chromatin Remodelling. *Nat. Rev. Mol. Cell Biol.* 2017, 18, 610–621.
- Hoch, N.C.; Polo, L.M. ADP-Ribosylation: From Molecular Mechanisms to Human Disease. *Genet. Mol. Biol.* 2020, 43, e20190075.

8. Benjamin, R.C.; Gill, D.M. ADP-Ribosylation in Mammalian Cell Ghosts. Dependence of Poly(ADP-Ribose) Synthesis on Strand Breakage in DNA. *J. Biol. Chem.* 1980, 255, 10493–10501.
9. Durkacz, B.W.; Omidiji, O.; Gray, D.A.; Shall, S. (ADP-Ribose)<sub>n</sub> Participates in DNA Excision Repair. *Nature* 1980, 283, 593–596.
10. Dockery, L.; Gunderson, C.; Moore, K. Rucaparib: The Past, Present, and Future of a Newly Approved PARP Inhibitor for Ovarian Cancer. *OncoTargets Ther.* 2017, 10, 3029–3037.
11. Fong, P.C.; Boss, D.S.; Yap, T.A.; Tutt, A.; Wu, P.; Mergui-Roelvink, M.; Mortimer, P.; Swaisland, H.; Lau, A.; O'Connor, M.J.; et al. Inhibition of Poly(ADP-Ribose) Polymerase in Tumors from BRCA Mutation Carriers. *N. Engl. J. Med.* 2009, 361, 123–134.
12. Fong, P.C.; Yap, T.A.; Boss, D.S.; Carden, C.P.; Mergui-Roelvink, M.; Gourley, C.; De Greve, J.; Lubinski, J.; Shanley, S.; Messiou, C.; et al. Poly(ADP)-Ribose Polymerase Inhibition: Frequent Durable Responses in BRCA Carrier Ovarian Cancer Correlating With Platinum-Free Interval. *J. Clin. Oncol.* 2010, 28, 2512–2519.
13. Lin, K.K.; Harrell, M.I.; Oza, A.M.; Oaknin, A.; Ray-Coquard, I.; Tinker, A.V.; Helman, E.; Radke, M.R.; Say, C.; Vo, L.-T.; et al. BRCA Reversion Mutations in Circulating Tumor DNA Predict Primary and Acquired Resistance to the PARP Inhibitor Rucaparib in High-Grade Ovarian Carcinoma. *Cancer Discov.* 2019, 9, 210–219.
14. Tuli, R.; Shiao, S.L.; Nissen, N.; Tighiouart, M.; Kim, S.; Osipov, A.; Bryant, M.; Ristow, L.; Placencio-Hickok, V.; Hoffmann, D.; et al. A Phase 1 Study of Veliparib, a PARP-1/2 Inhibitor, with Gemcitabine and Radiotherapy in Locally Advanced Pancreatic Cancer. *EBioMedicine* 2019, 40, 375–381.
15. O'Connor, M.J. Targeting the DNA Damage Response in Cancer. *Mol. Cell* 2015, 60, 547–560.
16. Hassa, P.O. The Diverse Biological Roles of Mammalian PARPS, a Small but Powerful Family of Poly-ADP-Ribose Polymerases. *Front. Biosci.* 2008, 13, 3046.
17. Cho, C.C.; Chien, C.Y.; Chiu, Y.C.; Lin, M.H.; Hsu, C.H. Structural and Biochemical Evidence Supporting Poly ADP-Ribosylation in the Bacterium *Deinococcus Radiodurans*. *Nat. Commun.* 2019, 10, 14.
18. Mennella, M.R.F. The Dichotomy of the Poly(ADP-Ribose) Polymerase-Like Thermozyyme from *Sulfolobus Solfataricus*. *Challenges* 2018, 9, 5.
19. Nishizuka, Y.; Ueda, K.; Nakazawa, K.; Hayaishi, O. Studies on the Polymer of Adenosine Diphosphate Ribose. *J. Biol. Chem.* 1967, 242, 3164–3171.
20. Fujimura, S.; Hasegawa, S.; Shimizu, Y.; Sugimura, T. Polymerization of the Adenosine 5'-Diphosphate-Ribose Moiety of Nicotinamide-Adenine Dinucleotide by Nuclear Enzyme. I. Enzymatic Reactions. *Biochim. Biophys. Acta* 1967, 145, 247–259.
21. Ueda, K.; Reeder, R.H.; Honjo, T.; Nishizuka, Y.; Hayaishi, O. Poly Adenosine Diphosphate Ribose Synthesis Associated with Chromatin. *Biochem. Biophys. Res. Commun.* 1968, 31, 379–385.
22. Chambon, P.; Weill, J.D.; Doly, J.; Strosser, M.T.; Mandel, P. On the Formation of a Novel Adenylic Compound by Enzymatic Extracts of Liver Nuclei. *Biochem. Biophys. Res. Commun.* 1966, 25, 638–643.
23. Yamada, M.; Miwa, M.; Sugimura, T. Studies on Poly (Adenosine Diphosphate-Ribose) X. Properties of a Partially Purified Poly (Adenosine Diphosphate-Ribose) Polymerase'. *Arch. Biochem. Biophys.* 1971, 146, 579–586.
24. Juarez-Salinas, H.; Sims, J.L.; Jacobson, M.K. Poly(ADP-Ribose) Levels in Carcinogen-Treated Cells. *Nature* 1979, 282, 740–741.
25. Otake, H.; Miwa, M.; Fujimura, S.; Sugimura, T. Binding of ADP-ribose polymer with histone. *J. Biochem.* 1969, 65.
26. Wang, Z.Q.; Auer, B.; Stingl, L.; Berghammer, H.; Haidacher, D.; Schweiger, M.; Wagner, E.F. Mice Lacking ADPRT and Poly(ADP-Ribosyl)ation Develop Normally but Are Susceptible to Skin Disease. *Genes Dev.* 1995, 9, 509–520.
27. De Murcia, J.M.; Niedergang, C.; Trucco, C.; Ricoul, M.; Dutrillaux, B.; Mark, M.; Oliver, F.J.; Masson, M.; Dierich, A.; LeMeur, M.; et al. Requirement of Poly(ADP-Ribose) Polymerase in Recovery from DNA Damage in Mice and in Cells. *Proc. Natl. Acad. Sci. USA* 1997, 94, 7303–7307.
28. Masutani, M.; Suzuki, H.; Kamada, N.; Watanabe, M.; Ueda, O.; Nozaki, T.; Jishage, K.-I.; Watanabe, T.; Sugimoto, T.; Nakagama, H.; et al. Poly(ADP-Ribose) Polymerase Gene Disruption Conferred Mice Resistant to Streptozotocin-Induced Diabetes. *Proc. Natl. Acad. Sci. USA* 1999, 96, 2301–2304.
29. D'Amours, D.; Desnoyers, S.; D'Silva, I.; Poirier, G.G. Poly(ADP-Ribosyl)ation Reactions in the Regulation of Nuclear Functions. *Biochem. J.* 1999, 342, 249–268.
30. Schreiber, V.; Dantzer, F.; Ame, J.-C.; de Murcia, G. Poly(ADP-Ribose): Novel Functions for an Old Molecule. *Nat. Rev. Mol. Cell Biol.* 2006, 7, 517–528.

31. Hakmé, A.; Wong, H.; Dantzer, F.; Schreiber, V. The Expanding Field of Poly(ADP-ribose)ylation Reactions. *EMBO Rep.* 2008, 9, 1094–1100.
32. Langelier, M.-F.; Servent, K.M.; Rogers, E.E.; Pascal, J.M. A Third Zinc-Binding Domain of Human Poly(ADP-Ribose) Polymerase-1 Coordinates DNA-Dependent Enzyme Activation. *J. Biol. Chem.* 2008, 283, 4105–4114.
33. Langelier, M.-F.; Ruhl, D.D.; Planck, J.L.; Kraus, W.L.; Pascal, J.M. The Zn<sup>3</sup> Domain of Human Poly(ADP-Ribose) Polymerase-1 (PARP-1) Functions in Both DNA-Dependent Poly(ADP-Ribose) Synthesis Activity and Chromatin Compaction\*. *J. Biol. Chem.* 2010, 285, 18877–18887.
34. Langelier, M.-F.; Planck, J.L.; Roy, S.; Pascal, J.M. Structural Basis for DNA Damage-Dependent Poly(ADP-Ribosyl)ation by Human PARP-1. *Science* 2012, 336, 728–732.
35. Amé, J.-C.; Rolli, V.; Schreiber, V.; Niedergang, C.; Apiou, F.; Decker, P.; Muller, S.; Höger, T.; Murcia, J.M.; de Murcia, G. PARP-2, a Novel Mammalian DNA Damage-Dependent Poly(ADP-Ribose) Polymerase. *J. Biol. Chem.* 1999, 274, 17860–17868.
36. Léger, K.; Bär, D.; Savić, N.; Santoro, R.; Hottiger, M.O. ARTD2 Activity Is Stimulated by RNA. *Nucleic Acids Res.* 2014, 42, 5072–5082.
37. Brady, P.N.; Goel, A.; Johnson, M.A. Poly(ADP-Ribose) Polymerases in Host-Pathogen Interactions, Inflammation, and Immunity. *Microbiol. Mol. Biol. Rev.* 2018, 83.
38. Aravind, L.; Koonin, E.V. SAP—A Putative DNA-Binding Motif Involved in Chromosomal Organization. *Trends Biochem. Sci.* 2000, 25, 112–114.
39. Song, J.; Keppler, B.D.; Wise, R.R.; Bent, A.F. PARP2 Is the Predominant Poly(ADP-Ribose) Polymerase in Arabidopsis DNA Damage and Immune Responses. *PLoS Genet.* 2015, 11, e1005200.
40. Rissel, D.; Peiter, E. Poly(ADP-Ribose) Polymerases in Plants and Their Human Counterparts: Parallels and Peculiarities. *Int. J. Mol. Sci.* 2019, 20, 1638.
41. Okubo, S.; Hara, F.; Tsuchida, Y.; Shimotakahara, S.; Suzuki, S.; Hatanaka, H.; Yokoyama, S.; Tanaka, H.; Yasuda, H.; Shindo, H. NMR Structure of the N-Terminal Domain of SUMO Ligase PIAS1 and Its Interaction with Tumor Suppressor P53 and A/T-Rich DNA Oligomers. *J. Biol. Chem.* 2004, 279, 31455–31461.
42. Riccio, A.A.; Cingolani, G.; Pascal, J.M. PARP-2 Domain Requirements for DNA Damage-Dependent Activation and Localization to Sites of DNA Damage. *Nucleic Acids Res.* 2016, 44, 1691–1702.
43. The PyMOL Molecular Graphics System; Schrödinger, LLC: New York, NY, USA, 2021.
44. Sievers, F.; Wilm, A.; Dineen, D.; Gibson, T.J.; Karplus, K.; Li, W.; Lopez, R.; McWilliam, H.; Remmert, M.; Söding, J.; et al. Fast, Scalable Generation of High-Quality Protein Multiple Sequence Alignments Using Clustal Omega. *Mol. Syst. Biol.* 2011, 7, 539.
45. Madeira, F.; Park, Y.M.; Lee, J.; Buso, N.; Gur, T.; Madhusoodanan, N.; Basutkar, P.; Tivey, A.R.N.; Potter, S.C.; Finn, R.D.; et al. The EMBL-EBI Search and Sequence Analysis Tools APIs in 2019. *Nucleic Acids Res.* 2019, 47, W636–W641.
46. Ruf, A.; de Murcia, J.M.; de Murcia, G.; Schulz, G.E. Structure of the Catalytic Fragment of Poly(ADP-Ribose) Polymerase from Chicken. *Proc. Natl. Acad. Sci. USA* 1996, 93, 7481–7485.
47. Ruf, A.; de Murcia, G.; Schulz, G.E. Inhibitor and NAD<sup>+</sup> Binding to Poly(ADP-Ribose) Polymerase As Derived from Crystal Structures and Homology Modeling †, ‡. *Biochemistry* 1998, 37, 3893–3900.
48. Ruf, A.; Rolli, V.; de Murcia, G.; Schulz, G.E. The Mechanism of the Elongation and Branching Reaction of Poly(ADP-Ribose) Polymerase as Derived from Crystal Structures and Mutagenesis. *J. Mol. Biol.* 1998, 278, 57–65.
49. Oliver, A.W.; Amé, J.-C.; Roe, S.M.; Good, V.; de Murcia, G.; Pearl, L.H. Crystal Structure of the Catalytic Fragment of Murine Poly(ADP-Ribose) Polymerase-2. *Nucleic Acids Res.* 2004, 32, 456–464.
50. Kinoshita, T.; Nakanishi, I.; Warizaya, M.; Iwashita, A.; Kido, Y.; Hattori, K.; Fujii, T. Inhibitor-Induced Structural Change of the Active Site of Human Poly(ADP-Ribose) Polymerase. *FEBS Lett.* 2004, 556, 43–46.
51. Karlberg, T.; Hammarström, M.; Schütz, P.; Svensson, L.; Schüler, H. Crystal Structure of the Catalytic Domain of Human PARP2 in Complex with PARP Inhibitor ABT-888. *Biochemistry* 2010, 49, 1056–1058.
52. Lehtiö, L.; Jemth, A.-S.; Collins, R.; Loseva, O.; Johansson, A.; Markova, N.; Hammarström, M.; Flores, A.; Holmberg-Schiavone, L.; Weigelt, J.; et al. Structural Basis for Inhibitor Specificity in Human Poly(ADP-Ribose) Polymerase-3 †. *J. Med. Chem.* 2009, 52, 3108–3111.
53. Bilokapic, S.; Suskiewicz, M.J.; Ahel, I.; Halic, M. Bridging of DNA Breaks Activates PARP2–HPF1 to Modify Chromatin. *Nature* 2020, 585, 609–613.

54. Caldecott, K.W. Single-Strand Break Repair and Genetic Disease. *Nat. Rev. Genet.* 2008, 9, 619–631.
55. White, R.R.; Vijg, J. Do DNA Double-Strand Breaks Drive Aging? *Mol. Cell* 2016, 63, 729–738.
56. Silva, E.; Ideker, T. Transcriptional Responses to DNA Damage. *DNA Repair* 2019, 79, 40–49.
57. Langelier, M.-F.; Riccio, A.A.; Pascal, J.M. PARP-2 and PARP-3 Are Selectively Activated by 5' Phosphorylated DNA Breaks Through an Allosteric Regulatory Mechanism Shared with PARP-1. *Nucleic Acids Res.* 2014, 42, 7762–7775.
58. Hiom, K. Coping with DNA Double Strand Breaks. *DNA Repair* 2010, 9, 1256–1263.
59. Caldecott, K.W. XRCC1 Protein; Form and Function. *DNA Repair* 2019, 81, 102664.
60. Das, B.B.; Huang, S.N.; Murai, J.; Rehman, I.; Amé, J.-C.; Sengupta, S.; Das, S.K.; Majumdar, P.; Zhang, H.; Biard, D.; et al. PARP1–TDP1 Coupling for the Repair of Topoisomerase I–Induced DNA Damage. *Nucleic Acids Res.* 2014, 42, 4435–4449.
61. Spagnolo, L.; Barbeau, J.; Curtin, N.J.; Morris, E.P.; Pearl, L.H. Visualization of a DNA-PK/PARP1 Complex. *Nucleic Acids Res.* 2012, 40, 4168–4177.
62. Roth, D.B. V(D)J Recombination: Mechanism, Errors, and Fidelity. In *Mobile DNA III*; John Wiley & Sons: Hoboken, NJ, USA, 2015.
63. Haince, J.-F.; Kozlov, S.; Dawson, V.L.; Dawson, T.M.; Hendzel, M.J.; Lavin, M.F.; Poirier, G.G. Ataxia Telangiectasia Mutated (ATM) Signaling Network Is Modulated by a Novel Poly(ADP-Ribose)-Dependent Pathway in the Early Response to DNA-Damaging Agents. *J. Biol. Chem.* 2007, 282, 16441–16453.
64. Aguilar-Quesada, R.; Muñoz-Gámez, J.; Martín-Oliva, D.; Peralta, A.; Valenzuela, M.T.; Matínez-Romero, R.; Quiles-Pérez, R.; Murcia, J.; de Murcia, G.; de Almodóvar, M.; et al. Interaction between ATM and PARP-1 in Response to DNA Damage and Sensitization of ATM Deficient Cells Through PARP Inhibition. *BMC Mol. Biol.* 2007, 8, 29.
65. Haince, J.-F.; McDonald, D.; Rodrigue, A.; Déry, U.; Masson, J.-Y.; Hendzel, M.J.; Poirier, G.G. PARP1-Dependent Kinetics of Recruitment of MRE11 and NBS1 Proteins to Multiple DNA Damage Sites. *J. Biol. Chem.* 2008, 283, 1197–1208.
66. Grabarz, A.; Barascu, A.; Guirouilh-Barbat, J.; Lopez, B.S. Initiation of DNA Double Strand Break Repair: Signaling and Single-Stranded Resection Dictate the Choice Between Homologous Recombination, Non-Homologous End-Joining and Alternative End-Joining. *Am. J. Cancer Res.* 2012, 2, 249–268.
67. Langelier, M.-F.; Planck, J.L.; Roy, S.; Pascal, J.M. Crystal Structures of Poly(ADP-Ribose) Polymerase-1 (PARP-1) Zinc Fingers Bound to DNA: Structural and Functional Insights into DNA-Dependent PARP-1 Activity. *J. Biol. Chem.* 2011, 286, 10690–10701.
68. Ali, A.A.E.; Timinszky, G.; Arribas-Bosacoma, R.; Kozłowski, M.; Hassa, P.O.; Hassler, M.; Ladurner, A.G.; Pearl, L.H.; Oliver, A.W. The Zinc-Finger Domains of PARP1 Cooperate to Recognize DNA Strand Breaks. *Nat. Struct. Mol. Biol.* 2012, 19, 685–692.
69. Eustermann, S.; Wu, W.-F.; Langelier, M.-F.; Yang, J.-C.; Easton, L.E.; Riccio, A.A.; Pascal, J.M.; Neuhaus, D. Structural Basis of Detection and Signaling of DNA Single-Strand Breaks by Human PARP-1. *Mol. Cell* 2015, 60, 742–754.
70. Obaji, E.; Haikarainen, T.; Lehtiö, L. Structural Basis for DNA Break Recognition by ARTD2/PARP2. *Nucleic Acids Res.* 2018, 46, 12154–12165.
71. Eustermann, S.; Videler, H.; Yang, J.-C.; Cole, P.T.; Gruszka, D.; Veprintsev, D.; Neuhaus, D. The DNA-Binding Domain of Human PARP-1 Interacts with DNA Single-Strand Breaks as a Monomer through Its Second Zinc Finger. *J. Mol. Biol.* 2011, 407, 149–170.
72. Trucco, C.; Flatter, E.; Fribourg, S.; de Murcia, G.; Ménissier-de Murcia, J. Mutations in the Amino-Terminal Domain of the Human Poly(ADP-Ribose) Polymerase That Affect Its Catalytic Activity but Not Its DNA Binding Capacity. *FEBS Lett.* 1996, 399, 313–316.
73. Rulten, S.L.; Fisher, A.E.O.; Robert, I.; Zuma, M.C.; Rouleau, M.; Ju, L.; Poirier, G.; Reina-San-Martin, B.; Caldecott, K.W. PARP-3 and APLF Function Together to Accelerate Nonhomologous End-Joining. *Mol. Cell* 2011, 41, 33–45.
74. Zarkovic, G.; Belousova, E.A.; Talhaoui, I.; Saint-Pierre, C.; Kutuzov, M.M.; Matkarimov, B.T.; Biard, D.; Gasparutto, D.; Lavrik, O.I.; Ishchenko, A.A. Characterization of DNA ADP-Ribosyltransferase Activities of PARP2 and PARP3: New Insights into DNA ADP-Ribosylation. *Nucleic Acids Res.* 2018, 46, 2417–2431.
75. Liu, L.; Kong, M.; Gassman, N.R.; Freudenthal, B.D.; Prasad, R.; Zhen, S.; Watkins, S.C.; Wilson, S.H.; Van Houten, B. PARP1 Changes from Three-Dimensional DNA Damage Searching to One-Dimensional Diffusion after Auto-PARylation or in the Presence of APE1. *Nucleic Acids Res.* 2017, 45, 12834–12847.
76. Milo, R.; Jorgensen, P.; Moran, U.; Weber, G.; Springer, M. BioNumbers—the Database of Key Numbers in Molecular and Cell Biology. *Nucleic Acids Res.* 2010, 38, D750–D753.

77. Huber, M.D.; Gerace, L. The Size-Wise Nucleus: Nuclear Volume Control in Eukaryotes. *J. Cell. Biol.* 2007, 179, 583–584.
  78. Sukhanova, M.V.; Abrakhi, S.; Joshi, V.; Pastre, D.; Kutuzov, M.M.; Anarbaev, R.O.; Curmi, P.A.; Hamon, L.; Lavrik, O.I. Single Molecule Detection of PARP1 and PARP2 Interaction with DNA Strand Breaks and Their Poly(ADP-Ribosyl)ation Using High-Resolution AFM Imaging. *Nucleic Acids Res.* 2016, 44, e60.
  79. Sukhanova, M.V.; Hamon, L.; Kutuzov, M.M.; Joshi, V.; Abrakhi, S.; Dobra, I.; Curmi, P.A.; Pastre, D.; Lavrik, O.I. A Single-Molecule Atomic Force Microscopy Study of PARP1 and PARP2 Recognition of Base Excision Repair DNA Intermediates. *J. Mol. Biol.* 2019, 431, 2655–2673.
  80. Rudolph, J.; Mahadevan, J.; Dyer, P.; Luger, K. Poly(ADP-Ribose) Polymerase 1 Searches DNA via a ‘Monkey Bar’ Mechanism. *eLife* 2018, 7, e37818.
  81. Rudolph, J.; Mahadevan, J.; Luger, K. Probing the Conformational Changes Associated with DNA Binding to PARP1. *Biochemistry* 2020, 59, 2003–2011.
- 

Retrieved from <https://encyclopedia.pub/entry/history/show/32324>